WATER RESOURCES RESEARCH, VOL. 49, 1211–1225, doi:10.1002/wrcr.20120, 2013

# Multiobjective optimization of water distribution systems accounting for economic cost, hydraulic reliability, and greenhouse gas emissions

Wenyan Wu,[1] Holger R. Maier,[1] and Angus R. Simpson[1]

Received 12 May 2012; revised 24 January 2013; accepted 29 January 2013; published 1 March 2013.

[1] In this paper, three objectives are considered for the optimization of water distribution systems (WDSs): the traditional objectives of minimizing economic cost and maximizing hydraulic reliability and the recently proposed objective of minimizing greenhouse gas (GHG) emissions. It is particularly important to include the GHG minimization objective for WDSs involving pumping into storages or water transmission systems (WTSs), as these systems are the main contributors of GHG emissions in the water industry. In order to better understand the nature of tradeoffs among these three objectives, the shape of the solution space and the location of the Pareto-optimal front in the solution space are investigated for WTSs and WDSs that include pumping into storages, and the implications of the interaction between the three objectives are explored from a practical design perspective. Through three case studies, it is found that the solution space is a U-shaped curve rather than a surface, as the tradeoffs among the three objectives are dominated by the hydraulic reliability objective. The Pareto-optimal front of real-world systems is often located at the "elbow" section and lower "arm" of the solution space (i.e., the U-shaped curve), indicating that it is more economic to increase the hydraulic reliability of these systems by increasing pipe capacity (i.e., pipe diameter) compared to increasing pumping power. Solutions having the same GHG emission level but different cost-reliability tradeoffs often exist. Therefore, the final decision needs to be made in conjunction with expert knowledge and the specific budget and reliability requirements of the system.

**Citation:** Wu, W., H. R. Maier, and A. R. Simpson (2013) Multiobjective optimization of water distribution systems accounting for economic cost, hydraulic reliability, and greenhouse gas emissions, *Water Resour. Res.*, *49*, 1211–1225, doi:10.1002/wrcr.20120.

## 1. Introduction

[2] The optimization of water distribution systems (WDSs) is a complex problem that usually has a large search space and multiple constraints. Traditionally, the WDS optimization problem has been treated as a single-objective problem with cost as the objective. This is because of the high cost associated with the construction and operation of these systems [*Simpson et al*., 1994]. More recently, it has been recognized that network reliability is also an important criterion in the design and operation of WDSs and should therefore be considered in addition to cost.

[3] In some of the earliest work on the reliability of WDSs, *Gessler and Walski* [1985] used the excess pressure at the worst node in the system as a measure of benefit in a pipe network optimization problem to ensure sufficient water with acceptable pressure is delivered to demand nodes. *Li et al*. [1993] extended network reliability analysis to include a portion of hydraulic reliability—the capacity reliability. This is defined as the probability that the carrying capacity of a network meets the demand. *Schneiter et al*. [1996] applied the concept of capacity reliability to a WDS optimal rehabilitation problem.

[4] References to the multiobjective optimization of WDSs accounting for network reliability can be traced back to the 1980s, when *Walski et al.* [1988] used the WADISO program to solve WDS pipe sizing problems considering both cost and the minimum pressure of the network. In a study by *Halhal et al*. [1997], the network cost and the total benefit (including the improvement in the pressure deficiencies in the network) were maximized. Since then, minimizing the head deficit at demand nodes has been used as a hydraulic capacity reliability measure in a number of multiobjective WDS optimization studies that considered both cost and system reliability [*Atiquzzaman et al*., 2006; *Jourdan et al*., 2005; *Keedwell and Khu*, 2004; *Savic*, 2002]. In 2000, *Todini* [2000] introduced a resilience index approach that was incorporated together with minimization of cost into multiobjective WDS optimization via a heuristic approach. The resilience index was used by *Farmani et al*. [2006] as a hydraulic reliability measure in a multiobjective WDS optimization problem considering cost, reliability, and water quality. Based on the resilience index, *Prasad and Park* [2004] introduced a network resilience measure and applied it to multiobjective genetic algorithm optimization of WDSs. Around the same time, *Tolson et al*. [2004] used a genetic algorithm coupled with the first-order

[1]School of Civil, Environmental and Mining Engineering, University of Adelaide, Adelaide, Australia.

Corresponding author: W. Wu, School of Civil, Environmental and Mining Engineering, University of Adelaide, Adelaide, 5005, Australia (wenyan.wu@adelaide.edu.au)


0043-1397/13/10.1002/wrcr.20120

reliability method (FORM) to obtain optimal tradeoffs between the cost and reliability of WDSs represented by the probability of failure. *Kapelan et al*. [2005] applied a multiobjective approach to maximize the robustness of a WDS, which was represented as the possibility that pressure heads at all network nodes are simultaneously equal to or above the minimum required pressure. *Jayaram and Srinivasan* [2008] modified the resilience index introduced by *Todini* [2000] and applied it to the optimal design and rehabilitation of WDSs via a multiobjective genetic algorithm approach. More recently, *Fu and Kapelan* [2011] used a fuzzy random reliability measure, which is defined as the probability that the fuzzy head requirements are satisfied across all network nodes, for the design of WDSs. *Fu et al*. [2012] developed a nodal hydraulic failure index to account for both nodal and tank failure in multiobjective WDS optimization.

[5] In the last 10 years, objectives focused on environmental considerations have started to be included in WDS optimization studies due to increased awareness of climate change, especially global warming. *Dandy et al*. [2006] used a single-objective approach to minimize the material usage, embodied energy, and greenhouse gas (GHG) emissions associated with the manufacture of PVC pipes. *Wu et al*. [2008] first introduced GHG emission minimization as an objective into the multiobjective optimal design of WDSs. Since then, a number of other WDS optimization studies have focused on the incorporation of GHG emissions associated with energy consumption into WDS optimization studies [*Dandy et al*., 2008; *Herstein et al*., 2009; *Wu et al*., 2010a, 2010b, 2012b]. It should be noted that there were a large number of earlier studies that included the minimization of energy consumption as an objective in WDS optimization [see *Ormsbee and Lansey*, 1994; *Pezeshk and Helweg*, 1996; *Nitivattananon et al*., 1996; *Ilich and Simonovic*, 1998; *van Zyl et al*., 2004; *Ulanicki et al.,* 2007]. However, these studies focused on the minimization of energy consumption as a means of cost minimization [*Ghimire and Barkdoll*, 2007], rather than the explicit minimization of environmental impacts.

[6] As can be seen from previous research, economic cost, hydraulic reliability, and environmental impact, especially in terms of GHG emissions, are important design criteria for WDSs. However, while there have been a number of studies that have considered the tradeoffs between cost and reliability and cost and GHG emissions, there have been no studies that have investigated the optimal tradeoffs between all of these three objectives. One reason for this is that traditionally used measures of hydraulic reliability cannot be used as an objective in WDSs where pumping into storages plays a major role. This is because the calculation of the majority of these hydraulic reliability measures relies upon the difference between the required and minimum allowable pressure heads at the outlet of the system, which is generally equal to a constant value of zero in these pumping systems [*Wu et al*., 2011], and can therefore not be used as an objective function. However, it is precisely these systems that are of most interest from a GHG emission minimization perspective, as they often require most pumping energy.

[7] The surplus power factor hydraulic reliability/resilience measure, which was introduced by *Vaabel et al*. [2006], overcomes the shortcoming of existing hydraulic reliability measures outlined above, as it can be used as an objective function in the optimization of water transmission systems (WTSs), which generally include pumping into storages. This is because calculation of the surplus power factor does not require the value of the pressure head at the outlet of the system. Consequently, this resilience measure is the only network hydraulic reliability measure that can be used in conjunction with the objectives of cost and GHG emission minimization for all types of networks, and particularly those that are of most interest from a GHG minimization perspective, such as transmission networks that pump water into storage facilities. As a result, this measure can be used in all studies considering cost, hydraulic reliability, and GHG emissions as objectives. The application of the surplus power factor as a hydraulic reliability measure for WDS optimization can be found in the study by *Wu et al*. [2011].

[8] The tradeoffs between cost minimization, hydraulic reliability maximization, and GHG emission minimization are important. We are now moving into an era where the minimization of GHG emissions from WDSs is becoming increasingly important. Consequently, the main aim of this paper is to gain a good understanding of the generic nature of the tradeoffs between these objectives for systems that involve pumping into storage facilities. The specific objectives include (1) to investigate the shape of the solution space formed by the three objectives for WDSs involving pumping or WTSs, (2) to investigate the location of the Pareto-optimal front in the solution space for a number of case studies, and (3) to elicit generic guidelines that are useful from a practical perspective when optimizing WDSs using cost, hydraulic reliability, and GHG emissions as objective functions. The specific research objectives are achieved via three case studies, including two hypothetical case studies from the literature and one real-world case study.

[9] The remainder of this paper is organized as follows. The formulation of the proposed three-objective optimization problem and the method used to analyze the multiobjective optimal solutions obtained are both introduced in section 2. Then, the three case studies and associated assumptions are presented in section 3, followed by the optimization results and their discussion in section 4. Conclusions are then made.

## 2. Methodology

### 2.1. Multiobjective WDS Problem Formulation

[10] The WDS optimization problem presented in this paper is formulated as a multiobjective design problem, in which the best combination of the values for decision variables need to be determined in terms of certain objectives, such that a number of constraints are satisfied. As mentioned in section 1, the three objectives considered include (1) minimizing the total life cycle cost of the system, (2) maximizing the hydraulic reliability of the system, as represented by the resilience measure given by *Wu et al*. [2011], and (3) minimizing total life cycle GHG emissions [*Wu et al*., 2010a, 2010b, 2011]. Thus, the WDS optimization problem investigated in this paper can be expressed using the following equations [*Wu et al*., 2010a]:

$$\text{minimize} \quad \mathrm{OF}_1 = \mathrm{CC} + \mathrm{PRC} + \mathrm{OC}, \tag{1}$$

where CC, PRC, and OC are capital, pump refurbishment, and operating costs, respectively.

$$\text{maximize} \quad \text{OF}_2 = \min\{\mathbf{s}\}, \tag{2}$$

where $\mathbf{s}$ is the vector of the surplus power factor of all pipes in a network.

$$\text{minimize} \quad \text{OF}_3 = \text{CGHG} + \text{OGHG}, \tag{3}$$

where CGHG and OGHG are the capital and operating GHG emissions, respectively,

[11] subject to

$$\text{GF}_j \geq 0 \quad j = 1, 2, \ldots, p, \tag{4}$$

$$\text{HF}_k = 0 \quad k = 1, 2, \ldots, q, \tag{5}$$

and

$$\text{LB}_t \leq x_t \leq \text{UB}_t \quad t = 1, 2, \ldots, n, \tag{6}$$

where OF = objective functions; $n$ = the number of decision variables; GF = inequality constraint functions; $p$ = the number of inequality constraints; HF = equality constraint functions; $q$= the number of equality constraints; $x_t$ = the $t$th decision variable; and $\text{LB}_t$ and $\text{UB}_t$ are the lower and upper bounds of the $t$th decision variable, respectively.

[12] In this paper, the decision variables of the WDS optimization problem considered include pipe sizes, which often take discrete values. Consequently, equation (6) can be expressed as

$$x_t \in \{x_{t1}, x_{t2}, \ldots, x_{tl}\}, \tag{7}$$

where $\{x_{t1}, x_{t2}, \ldots, x_{tl}\}$ are the $l$ discrete values of the $t$th decision variable.

[13] The constraints of the WDS optimization problems considered in this paper mainly include hydraulic constraints, available options of decision variables, and case study specific constraints. Hydraulic constraints refer to the physical rules that a hydraulic system must obey, which include

[14] 1. Conservation of mass: The continuity of flow must be maintained at each node in the network.

[15] 2. Conservation of energy: The total head loss around a loop must be zero and the total head loss along a path must equal the difference between the water elevations at the two end reservoirs.

[16] The available options of decision variables include available diameters of pipes. The case study specific constraints considered in this study include minimum allowable pressures at demand nodes for a distribution network and required flows for a transmission network. Details of the methods used for the evaluation of the objective functions and case study specific constraints are given in sections 2.2 and 3, respectively.

### 2.2. Objective Function Evaluation

#### 2.2.1. Total Life Cycle Cost

[17] The total life cycle cost of a WDS considered in this paper includes capital costs (i.e., CC in equation (1)), operating costs (i.e., OC in equation (1)), and pump refurbishment costs (i.e., PRC in equation (1)) [*Wu et al*., 2010a]. The capital cost consists of pump station cost, initial pump cost, and pipe cost. Pump station cost and initial pump cost can be estimated based on the size of the pump, which is usually determined based on network configuration and peak-day demand [*Wu et al*., 2010a]. Pipe cost is a function of pipe diameter and corresponding pipe length. Operating costs mainly result from the electricity consumption of system operation related to pumping during the design life of the system. In this study, a design life of 100 years is assumed for pipes, which is consistent with the suggestion by the *Water Services Association of Australia* [2002]. Refurbishment costs considered in this study are mainly due to the maintenance of pumps, which are assumed to be refurbished every 20 years or four times during the design life of the system [*Wu et al*., 2010a]. The calculation of both operating cost and pump refurbishment cost requires present value analysis. In this study, a discount rate of 8% is used, which has been used in related studies [*Wu et al*., 2010a, 2010b, 2012a, 2012b].

[18] The annual electricity consumption (AEC) due to pumping can be calculated using the following equation:

$$\begin{aligned} \text{AEC} &= \frac{T_{\text{year}}}{N} \sum_{t=1}^{T} \frac{P(t)}{\eta(t)_{\text{motor}}} \times \Delta t \\ &= \frac{T_{\text{year}}}{N} \sum_{t=1}^{T} \frac{1}{1000} \frac{\gamma \times Q(t) \times H(t)}{\eta(t)_{\text{pump}} \times \eta(t)_{\text{motor}}} \times \Delta t, \end{aligned} \tag{8}$$

where $T_{\text{year}}$ is the time in a year; $N$ is the number of extended period simulation (EPS) considered in a year; $t$ is the time step (e.g., the time step in an EPS); $P(t)$ is the pump power (kW); $\gamma$ is the specific weight of water ($\text{N/m}^3$); $Q(t)$ is the pump flow ($\text{m}^3/\text{s}$); $H(t)$ is the pump head ($m$); $\eta(t)_{\text{pump}}$ and $\eta(t)_{\text{motor}}$ are the pump efficiency and motor efficiency, respectively; $T$ is the number of time steps; and $\Delta t$ is the duration of each time step (hours). In this study, a pump efficiency of 85% and a motor efficiency of 95%, which were used in previous similar studies [*Wu et al*., 2010b, 2012b], are assumed in the computation of the AEC for each pump. The annual operating cost can be calculated by multiplying the AEC (in kWh) by the average electricity tariff (in \$/kWh) of the corresponding year. In this paper, a base electricity tariff of \$0.14/kWh is used for the first year of the design period. From the second year of the design period and onward, the electricity tariff is assumed to increase at 3% per annum. The annual demand is assumed to be constant throughout the design life. A detailed discussion on the assumed electricity tariffs can be found in *Wu et al*. [2012a].

#### 2.2.2. Hydraulic Reliability

[19] As discussed in section 1, the network resilience measure introduced by *Wu et al*. [2011] is used here as a hydraulic reliability measure to enable the consideration of systems that are of most interest from the perspective of GHG emission minimization. This measure makes use of the concept of the surplus power factor ($s$), introduced by *Vaabel et al*. [2006], which can be used to measure the resilience of a network subject to failure conditions, and thus the hydraulic reliability of the network, on the basis of

both pressure and flow. As mentioned previously, as the calculation of the surplus power factor does not require the value of the pressure head at the outlet of the system, it can be used to measure the resilience, and thus the hydraulic reliability of a WDS involving delivery into storage facilities [*Wu et al*., 2011]. The *s* factor (i.e., *s* in equation (2)) developed by *Vaabel et al*. [2006] can be calculated using the following equation:

$$s = 1 - \frac{a+1}{a}\left[1 - \frac{1}{a+1}\frac{Q_{\text{in}}^{a}}{Q_{\text{max}}^{a}}\right]\frac{Q_{\text{in}}}{Q_{\text{max}}}, \tag{9}$$

where $a$ is the flow exponent, $Q_{\text{in}}$ is the flow in the pipe, and $Q_{\text{max}}$ is the flow that leads to the maximum value of output power, which can be calculated using the following equation:

$$Q_{\text{max}} = \left(\frac{H_{\text{in}}}{(a+1)c}\right)^{\frac{1}{a}}, \tag{10}$$

where $c$ is the resistance coefficient of the pipe and $H_{\text{in}}$ is the head at the inlet of the pipe. For a detailed derivation of the *s* factor, please refer to *Vaabel et al*. [2006].

[20] The value of *s* characterizes the hydraulic reliability of a WDS [*Vaabel et al*., 2006]. The range of the *s* factor is from 0 to 1. When *s* is equal to zero, the hydraulic system works at its maximum capacity. Under this condition, any leakage can result in hydraulic failure of the system in terms of meeting the needs of end water users, such as delivering enough water with sufficient pressure. As the value of the *s* factor increases, the resilience of the system to failure conditions increases, and so does the hydraulic reliability of the system. However, as long as the system delivers water to end users, the value of *s* cannot reach 1, as under such conditions the friction loss within the pipe will be equal to $H_{\text{in}}$, and there will be no flow in the pipe. In this study, the minimum *s* factor (where the *s* factors of all the individual pipes are considered) in a network is used as the hydraulic reliability measure.

[21] An important property of the *s* factor is that a zero *s* factor value is achieved when $Q_{\text{in}}$ is equal to $Q_{\text{max}}$. In addition, a single value of *s* can be obtained under two different conditions: one condition is $Q_{\text{in}}$ being less than $Q_{\text{max}}$ and its opposite condition is $Q_{\text{in}}$ being greater than $Q_{\text{max}}$ [*Vaabel et al*., 2006]. In the region where $Q_{\text{in}}$ is less than $Q_{\text{max}}$, the increase in hydraulic reliability or the *s* factor is driven by the increase in pipe hydraulic capacity, thus the pipe diameter; whereas, in the region where $Q_{\text{in}}$ is greater than $Q_{\text{max}}$, the increase in *s* factor is driven by the increase in power input to the system, which, in the case of WTSs, is the pumping power. This property of the *s* factor has been noted previously [*Wu et al*., 2011] and has a significant impact on the shape of the solution space and the location of the Pareto-optimal front, as discussed in sections 4.1 and 4.2.

#### 2.2.3. Total Life Cycle GHG Emissions

[22] In this study, the total life cycle GHG emissions of a WDS are due to energy consumption related to the fabrication and use stages of the life cycle of a WDS [*Wu et al*., 2010a]. The GHG emissions related to the energy consumption of the fabrication stage of a WDS are referred to as capital emissions (i.e., CGHG in equation (3)) [*Wu et al*., 2010a]. Only emissions from pipe manufacture are considered here as they represent the largest proportion of the impact [*Filion et al*., 2004]. In order to calculate the energy consumption during the fabrication stage of a WDS, embodied energy analysis (EEA) is first used to convert the mass of pipes to their equivalent embodied energy. In this study, an embodied energy factor for ductile iron cement-mortar lined (DICL) pipes of 40.2 MJ/kg is used. This value was estimated by *Ambrose et al*. [2002] based on a combination of published data and actual factory manufacturing data.

[23] Once the embodied energy consumption of a WDS is determined, emission factor analysis (EFA) is used to convert energy in megajoules into GHGs in kilograms of carbon dioxide equivalent ($CO_2$-e). In practice, emission factor values may vary across regions and with time, depending on the makeup of electricity energy sources (e.g., thermal, nuclear, wind, hydroelectricity, etc.). In this study, a base average emission factor of 0.98 kg $CO_2$-e/kWh is used for the first year of the design period, which was the full-fuel-cycle emission factor value of South Australia in 2007 [*The Department of Climate Change*, 2008]. Thereafter, the emission factor is assumed to decrease linearly to 70% of the 2007 level at the end of the design period of 100 years due to government policy of encouraging a move to cleaner energy in the form of renewable energy sources. The base emission factor is used to calculate capital emissions. A detailed discussion of the assumed GHG emission factors can be found in *Wu et al*. [2012a].

[24] GHG emissions due to system operation (i.e., OGHG in equation (3)) of pumping are assumed to account for the majority of emissions from the use stage of a WDS [*Wu et al*., 2010a]. The annual operating emissions are taken as the AEC (defined in equation (8)) multiplied by the average emission factor of the corresponding year. The operating emissions due to pumping also occur over time within the design period; however, no discounting (that is a discount rate of zero percent) is applied to the calculation of pumping GHG emissions based on the recommendation of the Intergovernmental Panel on Climate Change (IPCC) [*Fearnside*, 2002].

### 2.3. Analysis of Pareto-Optimal Solutions

[25] One big challenge of multiobjective optimization is the extraction of information that is useful for decision-making processes, as a result of the large number of optimal solutions that may be generated. Consequently, post-processing is often required in order to improve the effectiveness of the decision support information obtained [*Giustolisi et al*., 2006]. In this study, the concept of Pareto preference ordering developed by *Das* [1999] is used to reduce the number of eligible candidates in the final decision-making process and increase the effectiveness of the decision-supporting information that can be extracted from Pareto fronts.

[26] The concept of Pareto preference ordering was introduced to establish a hierarchical ordering system for various multicriteria alternatives that automatically identifies "inferior" solutions in a set of Pareto-optimal solutions. The concept is based on two definitions and a claim [*Das*, 1999]:

[27] **Definition 1:** For a multiobjective optimization problem considering *m* objectives, a Pareto-optimal solution

is defined as efficient of order $k$ (or a $k$-Pareto-optimal solution) ($1 \leq k \leq m$) if this solution is not dominated by any other solution in any of the $k$-dimensional subobjective spaces.

[28] **Definition 2:** For a multiobjective optimization problem considering $m$ objectives, a Pareto-optimal solution is defined to be of efficiency of order $k$ with degree $p$ (or a $[k,p]$-Pareto-optimal solution) if it is not dominated by any other points for exactly $p$ out of the possible $\binom{m}{k}$ $k$-dimensional subobjective spaces.

[29] **Claim:** If a solution is efficient of order $k$, it is efficient of order $j$ for any $j > k$.

[30] It can be seen from the definitions that the efficiency of order $m$ is the traditional concept of Pareto-optimality and the efficiency of order $k$, where ($1 \leq k \leq m$) is an extension of the traditional concept of Pareto-optimality. When there are a large number of solutions of efficiency of order $k$ (i.e., $k$-Pareto-optimal solutions), the concept of efficiency of order $k-1$ with degree $p$ can be used to find more desirable solutions. The higher the $p$ value, the closer the solution is to be efficient of order $k$, and it is more likely that the solution has "balanced" values of all objectives and thus is more desirable from a multiobjective point of view [*Das*, 1999]. By reducing the efficiency of order $k$ and increasing the degree $p$, the criteria of Pareto-optimality are tightened, and more desirable solutions can be identified. Pareto preference ordering can effectively reduce the number of candidate solutions in the final decision-making process and assist in identifying suitable solutions. Based on the claim, any Pareto-optimal solutions will still be Pareto-optimal when additional objectives are considered, and therefore, considering three objectives simultaneously in this study will not compromise the optimization considering any pair of the three objectives. Pareto preference ordering has been found to be able to help decision makers to find the desirable solutions that cannot be found in the Pareto-optimal set based on expert knowledge alone [*Khu and Madsen*, 2005].

## 3. Case Studies

### 3.1. Background

[31] Based on the previously stated objectives of the paper, three case studies are used to (1) investigate the shape of the solution space formed by the three objectives; (2) investigate the location of the Pareto-optimal front in the solution space; and (3) elicit generic guidelines that are useful from a practical perspective when optimizing WDSs using cost, hydraulic reliability, and GHG emissions as objective functions. The first case study is a hypothetical WTS, which has been adapted from *Wu et al*. [2010b]. It is a small system, which can be fully enumerated. Therefore, it is selected to analyze the solution space formed by the three objectives, the interaction of the three objectives, and the change in Pareto-optimality in the solution space in detail. The second case study is a hypothetical WDS selected from the literature. In the system, water is delivered into both a tank and demand nodes via a pump. The last case study is a real-world WTS from Australia. The second and third case studies are selected to investigate both the shape of the solution space and the location of the Pareto-optimal front, and explore the implications of the interactions among the three objectives for larger systems delivering water into storage facilities. Details of the three case studies and the optimization methods and parameters used are provided in the subsequent sections.

### 3.2. Case Study 1

[32] The first case study network has been adapted from *Wu et al*. [2010b], and consists of one source reservoir, one pump, one pipe of 1500 m, and one storage reservoir with an elevation (EL) of 95 m (i.e., EL 95 m). The average peak-day flow of the system is 120 L/s. DICL pipes of diameters between 200 and 1000 mm are finely discretized at 1 mm intervals and used as decision variable options in order to investigate the shape of the solution space in detail. Therefore, the entire solution space consists of a total of 801 networks. The unit cost and unit mass of these pipes are interpolated form the DICL pipe data reported in *Wu et al*. [2010a]. In order to account for pipe aging, four pipe roughness values (0.0015, 0.1, 0.5, 1.0 mm) are used, each of which is assumed to represent the average roughness of pipes of every consecutive 25 years of the 100 year design period.

### 3.3. Case Study 2

[33] The second case study is a WDS investigated by *Duan et al*. [1990]. In the original study by *Duan et al*. [1990], six reliability parameters were included in the single-objective design process as constraints. In contrast, in this study, these reliability constraints are replaced by the hydraulic reliability objective of maximizing the minimum $s$ factor in the network. This is possible because the $s$ factor can be used to measure the hydraulic reliability of a pumping system delivering water into reservoirs or storage tanks, which is the case in this network, as explained previously.

[34] The network configuration of the case study is shown in Figure 1. The network consists of 1 pump, 1 storage tank, 36 pipes and 16 demand nodes. The 24 h EPS with defined demands for every 6 h (i.e., 12 A.M. to 6 A.M., 6 A.M. to 12 P.M., 12 P.M. to 6 P.M. and 6 P.M. to 12 A.M.) used in the original study is also used in this study. In the first EPS time step, the pump needs to both supply the required demand and fill the tank completely; in the second EPS time step, demand is supplied by both the pump and tank; in the third EPS time step, the pump delivers the required demand and partially fills the tank that is drained

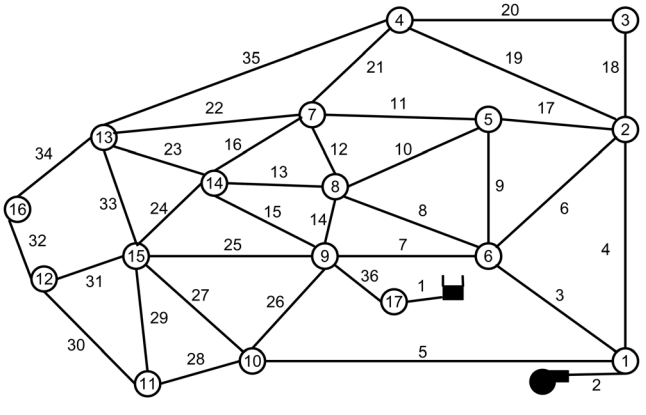


**Figure 1.** Network configuration of case study 2 (adapted from *Duan et al*. [1990]).

during the previous time step; while in the last time step of the EPS, demand again is supplied by both the pump and the tank. For details of the EPS, please refer to *Duan et al.* [1990]. The demands, nodal elevations, and pipe lengths in U.S. customary units in the original paper have been converted into SI units in this paper. The minimum head requirements at the demand nodes are 28.1 m (or 40 psi). The size of the pump is determined based on the network configurations evaluated in the optimization process [*Wu et al.*, 2010a]. Sixteen DICL pipes with diameters ranging from 100 to 1000 mm are used as decision variable options for the 36 pipes, resulting in a solution space of $16^{36}$ networks. Details of these pipes can be found in *Wu et al.* [2010a]. The same roughness values as in case study 1 are used.

### 3.4. Case Study 3

[35] The third case study is a real-world WTS in South Australia. The network configuration is shown in Figure 2. The system is responsible for delivering water into a service zone (Zone S in Figure 2) with a population of fewer than 5000 and an annual demand of 320 ML. Most of the connections in Zone S are residential, with only a few commercial connections and no major industrial connections.

[36] The network consists of one source reservoir (EL 146 m), two storage tanks (EL 95 m and EL 162 m, respectively), one pump station, and 20 major pipes. Water is directly fed into the EL 95 tank from the reservoir, and then pumped from the EL 95 tank into the EL 162 tank via a pump station, and supplies all of Zone S. The reservoir is also responsible for supplying water into a storage facility in Zone A with an average peak day demand of 750 L/s. However, Zone A does not have an impact on the pumping system of the network. There are also nine additional demand nodes along the transmission pipeline. The elevations and base demands of the nine demand nodes and the lengths of the 20 pipes are summarized in Tables 1 and 2, respectively. The 24 h peak day demand pattern is illustrated in Figure 3. The minimum pressure head required at the demand nodes is 20 m.

**Table 1.** Summary of Demand Nodes for Case Study 3

| Node | Elevation (m) | Base Demand (L/s) |
|---|---|---|
| 1 | 78.58 | 0.21 |
| 2 | 76.81 | 0.02 |
| 3 | 76.47 | 0.06 |
| 4 | 86.70 | 0.09 |
| 5 | 116.18 | 0.41 |
| 6 | 125.35 | 0.37 |
| 7 | 136.31 | 0.38 |
| 8 | 143.32 | 0.26 |
| 9 | 73.59 | 160.00 |

[37] For this case study, the peak day demand is used to evaluate constraints and the minimum $s$ factor of the network. The average day demand, which is calculated by dividing the peak day demand by the peak day factor of 1.5 [*Wu et al.*, 2010a], is used to calculate the energy consumption and thus the economic and environmental objective function values. As Zone S is an established distribution zone with little potential to grow, the current tank size (i.e., 38.22 m in diameter and 8 m in height) and tank trigger levels (i.e., 3.96 and 5.54 m) are used. The 20 main pipes along the transmission part of the network are considered as decision variables with the same 16 DICL pipes used by *Wu et al.* [2010a] as options, resulting in a total search space of $16^{20}$ networks. The size of the pump is determined based on the network configuration evaluated in the optimization process [*Wu et al.*, 2010a]. The four roughness values used for case study 1 are also used for this case study to account for pipe aging.

### 3.5. Optimization Methods

[38] In this study, the EPANET2 hydraulic model [*Rossman*, 2000] is used for the simulation of the networks in

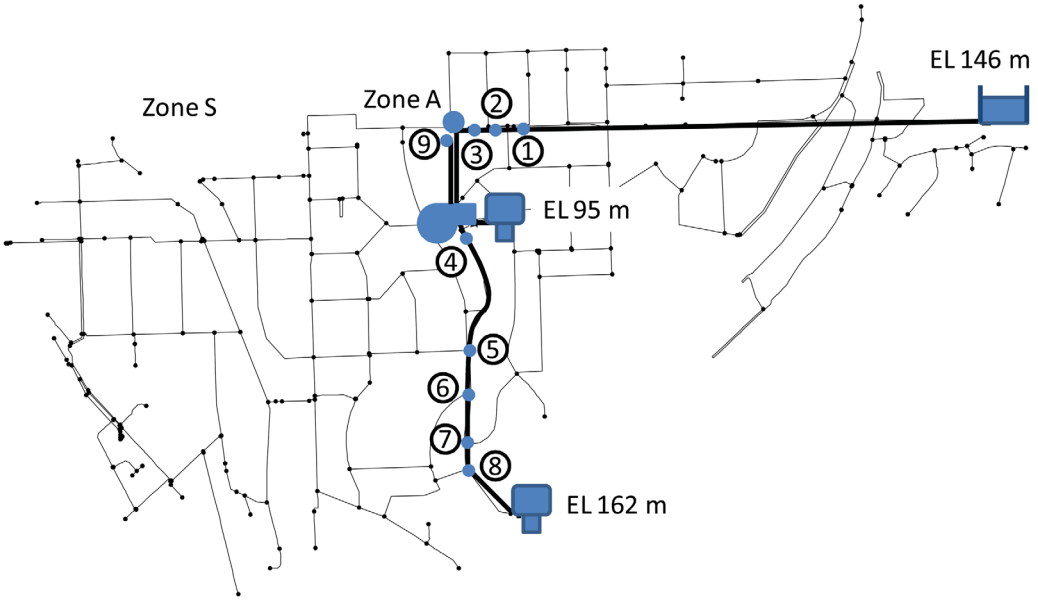


**Figure 2.** Network configuration of case study 3.

**Table 2.** Summary of Pipes for Case Study 3

| Pipe | Length (m) | Pipe | Length (m) |
|---|---|---|---|
| 1 | 1267.62 | 11 | 9.90 |
| 2 | 102.24 | 12 | 1.71 |
| 3 | 15.64 | 13 | 18.59 |
| 4 | 34.36 | 14 | 240.01 |
| 5 | 255.43 | 15 | 117.92 |
| 6 | 15.27 | 16 | 117.86 |
| 7 | 11.12 | 17 | 135.40 |
| 8 | 39.99 | 18 | 62.69 |
| 9 | 80.45 | 19 | 197.10 |
| 10 | 17.93 | 20 | 238.45 |

order to evaluate the objective functions of each network in the optimization process and to check whether constraints are satisfied. For the first case study, a full enumeration of the entire solution space has been carried out and therefore, the final solutions are the true Pareto-optimal solutions. For the second and third case studies, a multiobjective genetic algorithm called water system multiobjective genetic algorithm (WSMGA), which was developed by *Wu et al*. [2010a] based on the multiobjective genetic algorithm NSGA-II [*Deb et al*., 2000], is used to search for the Pareto-optimal solutions.

[39] For case studies 2 and 3, 50 separate multiobjective genetic algorithm optimization runs with different random seeds are conducted to ensure (near) Pareto-optimal solutions are found. Consequently, the resulting optimal front for each case study is formed from the best solutions found in the 50 optimization runs. A population size of 500, a maximum number of generations of 3000, a probability of crossover of 0.9, and a probability of mutation of 0.03 are used for the first case study; and a population size of 200, a maximum number of generations of 1200, a probability of crossover of 0.9, and a probability of mutation of 0.05 are used for the second case study. The population sizes and generation numbers are selected based on the results of a number of test runs. The crossover probability is selected based on previous experience with optimization using genetic algorithms. The mutation probability is selected based on both test runs and the following rule of thumb: the probability of mutation is approximately equal to one over the length of the chromosome (the number of bits representing one individual). With the above genetic algorithm parameters, each multiobjective genetic algorithm run requires 14 CPU hours for the second case study and 97 CPU hours for the third case study (2.66 GHz Intel Clovertown quad core processors), which results in a total of 5550 CPU hours to conduct the 50 runs for both case studies.

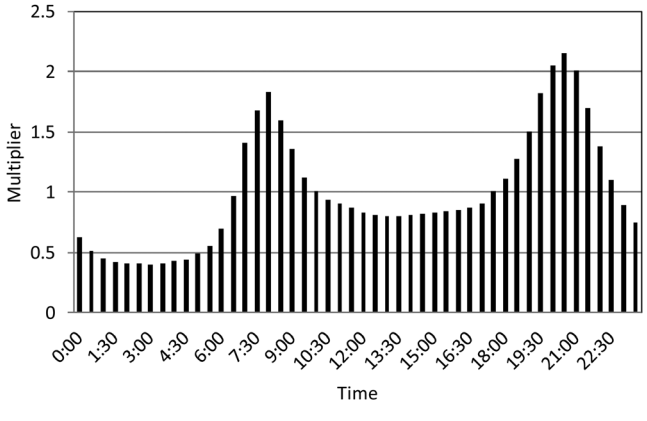


**Figure 3.** Diurnal water demand curve for case study 3.

## 4. Results and Discussion

### 4.1. Shape of the Solution Space

[40] In total, 687, 1313, and 337 Pareto-optimal solutions are found for case studies 1–3, respectively. The Pareto-optimal solutions for the three case studies and the solution space of case study 1 are plotted in Figure 4. Due to the large number of the Pareto-optimal solutions found, Pareto preference ordering (as outlined in section 2.3) is used to analyze the Pareto-optimal solutions and reduce the number of candidate solutions for further analysis. The results from the Pareto preference ordering for the three case studies are summarized in Tables 3–5, respectively.

[41] As can be seen from Figure 4, the solution space of case study 1 and the Pareto-optimal fronts for all three case studies are close to a curve rather than a surface in the three-dimensional (3-D) objective space. This indicates that in the majority of the solution space the tradeoffs among the three objectives are dominated by one objective. It is evident from Figure 4 that the Pareto-optimal fronts for all three cases are dominated by the hydraulic reliability of maximizing the minimum *s* factor in the network. This finding can be confirmed by the results shown in Tables 3–5, which show that the majority of the Pareto-optimal solutions are optimal in terms of the tradeoffs between the reliability objective and the other two objectives for all three case studies.

[42] In order to view the solution space and Pareto-optimal front more clearly, the solution space of case study 1 and the [2,3]- and [2,2]-Pareto-optimal solutions of all three case studies are plotted in Figure 5 from the less overlapped cost-GHG orientation of the objective space. It can be seen from Figure 5a that the solution space of case study 1 is a U-shaped curve that is roughly divided into three sections, the upper "arm," the "elbow" section, and the lower "arm" by the minimum cost solution and the minimum GHG solution. The minimum diameter solution (i.e., 200 mm) is located at the top of the upper "arm." The pipe diameter increases along the solution space form the top of the upper "arm" to the "elbow" section and to the maximum diameter solution (i.e., 1000 mm) located at the end of the lower "arm." The Pareto-optimal front is located on the "elbow" section and the lower "arm" of the solution space.

[43] Although the solution space of case studies 2 and 3 cannot be visualized as it is unknown due to its size, it can be seen from Figures 5b and 5c that the Pareto-optimal fronts of case studies 2 and 3 have a curved shape with an "elbow" section and a lower "arm" similar to the Pareto-optimal front of case study 1. The sizes of the pipes (represented by the cost of the pipes in the parentheses in Figures 5b and 5c) also increase along the Pareto-optimal front from the minimum cost solution located at the left end of the "elbow" section to the maximum *s* factor solution located at the right end of the lower "arm". This indicates that the solution spaces of case studies 2 and 3 have a similar shape to that of case study 1.

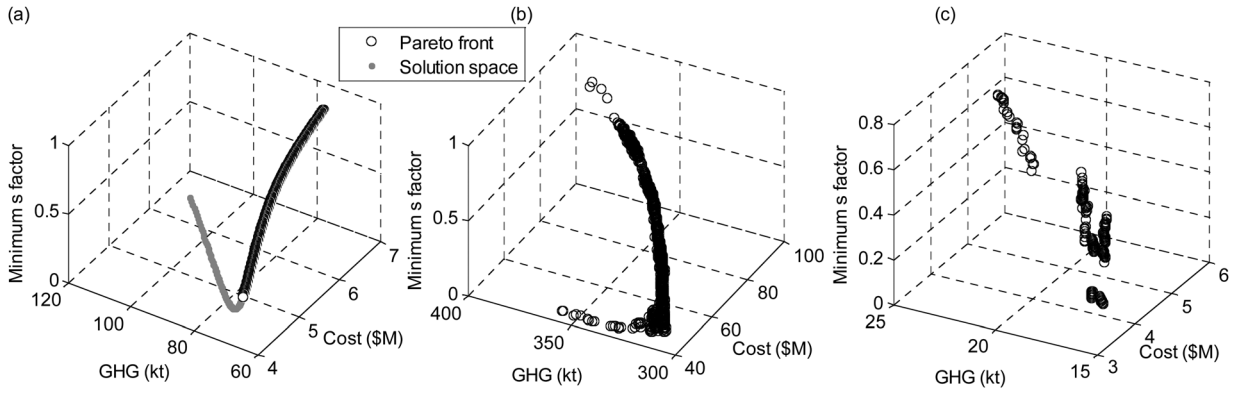


**Figure 4.** Pareto-optimal solutions of all case studies. (a) Case study 1 (EL 95) Pareto front and solution space, (b) Case study 2 Pareto front, and (c) Case study 3 Pareto front.

**Table 3.** Summary of Pareto Preference Ordering for Case Study 1 (EL 95)

| Pareto-Optimality | | Number of Solutions | Notes |
|---|---|---|---|
| [2,3]-Pareto-optimal solutions | | 1 | Minimum GHG solution |
| [2,2]-Pareto-optimal solutions | Cost-GHG and Cost-*s* optimal | 143 | Including minimum cost solution |
| | Cost-GHG and GHG-*s* optimal | 0 | |
| | Cost-*s* and GHG-*s* optimal | 543 | Including maximum *s* solution |
| [2,1]-Pareto-optimal solutions | Cost-GHG optimal | 0 | |
| | Cost-*s* optimal | 0 | |
| | GHG-*s* optimal | 0 | |

**Table 4.** Summary of Pareto Preference Ordering for Case Study 2

| Pareto-Optimality | | Number of Solutions | Notes |
|---|---|---|---|
| [2,3]-Pareto-optimal solutions | | 0 | |
| [2,2]-Pareto-optimal solutions | Cost-GHG and Cost-*s* optimal | 5 | Including minimum cost solution |
| | Cost-GHG and GHG-*s* optimal | 3 | Including minimum GHG solution |
| | Cost-*s* and GHG-*s* optimal | 74 | Including maximum *s* solution |
| [2,1]-Pareto-optimal solutions | Cost-GHG optimal | 38 | Including zero *s* solution |
| | Cost-*s* optimal | 328 | |
| | GHG-*s* optimal | 211 | |

**Table 5.** Summary of Pareto Preference Ordering for Case Study 3

| Pareto-Optimality | | Number of Solutions | Notes |
|---|---|---|---|
| [2,3]-Pareto-optimal solutions | | 0 | |
| [2,2]-Pareto-optimal solutions | Cost-GHG and Cost-*s* optimal | 2 | Including minimum cost solution |
| | Cost-GHG and GHG-*s* optimal | 1 | Including minimum GHG solution |
| | Cost-*s* and GHG-*s* optimal | 54 | Including maximum *s* solution |
| [2,1]-Pareto-optimal solutions | Cost-GHG optimal | 1 | |
| | Cost-*s* optimal | 73 | |
| | GHG-*s* optimal | 95 | |

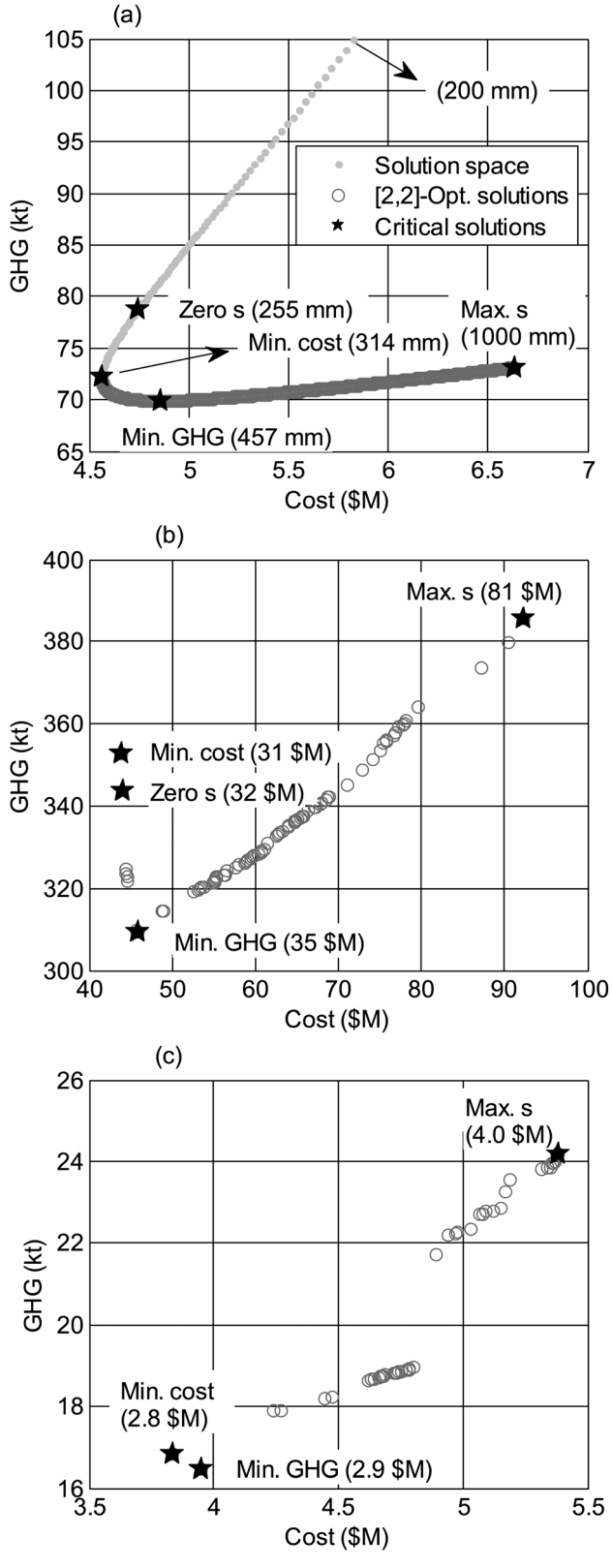


**Figure 5.** The [2,2]-Pareto-optimal solutions and critical solutions for all case studies from the cost-GHG orientation (Note: the number in the parentheses indicates the diameter of the pipe for case study 1 and the cost of pipes for case studies 2 and 3). Cost-GHG tradeoff: (a) case study 1 (EL 95), (b) case study 2, and (c) case study 3.

[44] The U shape of the solution space can be explained by the tradeoffs among the three objectives. The "elbow" section of the U shape is located between the minimum cost and minimum GHG solutions. The existence of the "elbow" section is mainly due to the tradeoffs between the economic and environmental objectives, which are largely determined by the discount rate used to calculate the economic cost [*Wu et al*., 2010a]. In other words, the "elbow" section of the solution space is the solution space of the traditional two-objective WDS optimization problem, considering the minimization of the economic cost and GHG emissions investigated in previous studies [*Wu et al*., 2010a, 2010b, 2012a, 2012b].

[45] The existence of the two "arms" of the solution space is due to the tradeoffs between the economic and environmental objectives and the hydraulic reliability objective of maximizing the *s* factor. As discussed in section 2.2.2, a single value of the *s* factor can be obtained under two different conditions: one where $Q_{in}$ is less than $Q_{max}$ and the other where $Q_{in}$ is greater than $Q_{max}$. The transition between these two conditions occurs when $Q_{in}$ is equal to $Q_{max}$ (i.e., at the zero *s* factor solution). As can be seen from Figure 5, the upper "arm" where the solutions have smaller pipes generally falls under the condition of $Q_{in}$ being greater than $Q_{max}$ and therefore higher *s* factor values are achieved by increased power input (e.g., pumping power). In contrast, the lower "arm," where the solutions have larger pipes, generally falls under the condition of $Q_{in}$ being less than $Q_{max}$ and therefore higher *s* factor values are achieved by increased pipe hydraulic capacity (i.e., pipe diameter).

[46] Based on the results for the three case studies, the shape of the solution space appears to be dominated by the choice of the *s* factor as the network reliability measure. However, as discussed in section 1, the *s* factor has to be used for systems where pumping into storages occurs, which are systems that are of most interest from a GHG emission minimization perspective. Therefore, the *s* factor should be used for problems that use cost minimization, hydraulic reliability maximization and GHG emission minimization as objectives in order to ensure that the same hydraulic reliability measure can be used for all problem types, enabling consistent results to be obtained. Consequently, the shape of the solution space obtained for the three case studies investigated here is likely to be generic for problems that consider these three objectives.

### 4.2. Location of Pareto-Optimal Front and Change in Pareto-Optimality

[47] The location of the Pareto-optimal front in the solution space is mainly determined by the tradeoffs between the hydraulic reliability objective of maximizing the *s* factor and the other two objectives. In order to illustrate how the location of the Pareto-front changes along the U-shaped solution space as a function of hydraulic reliability, different static heads ranging from 0 to 200 m are applied to case study network 1, and the 801 solutions with different pipe diameters are fully enumerated. It should be noted that different static heads (i.e., reservoir levels) result in different required power input or network hydraulic capacity in order to achieve certain hydraulic reliability levels as the *s* factor is directly related to the total power input required

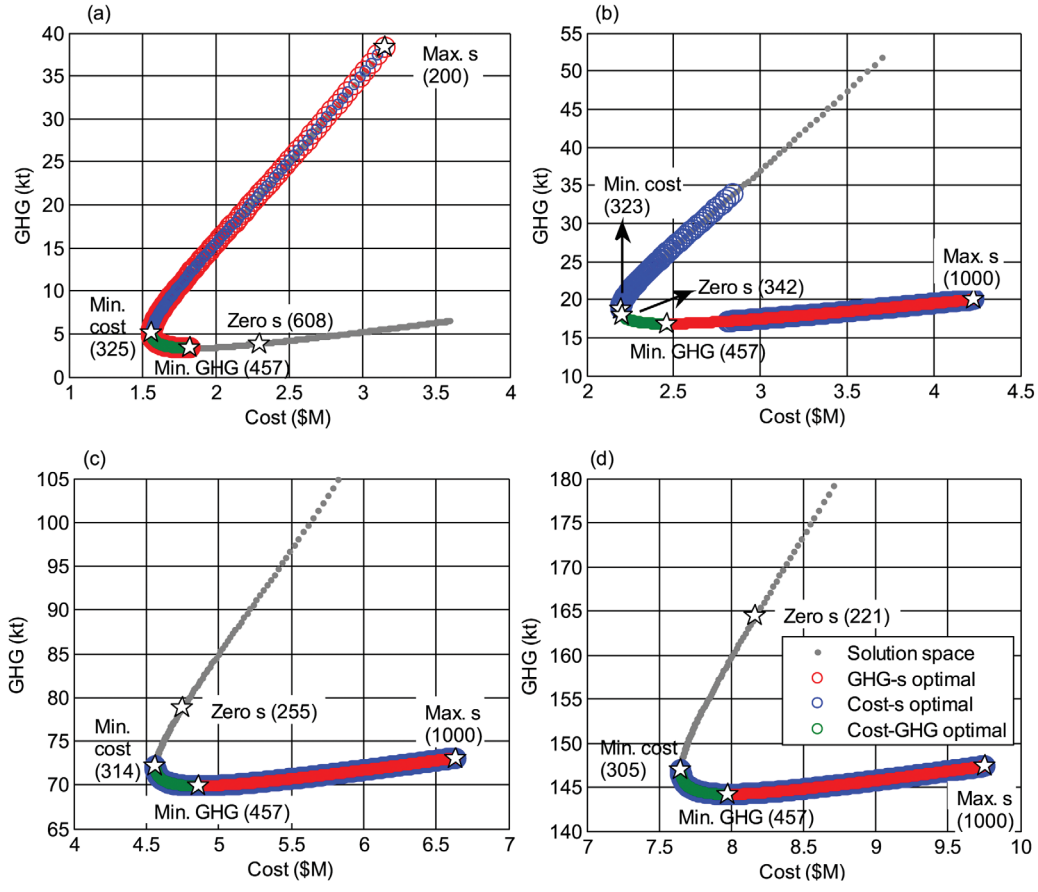


**Figure 6.** Solution space and two-objective optimality of Pareto-optimal solutions for case study 1 (Note: the number in parentheses indicates the diameter of the pipe). (a) EL1 (b) EL 20, (c) EL 95, and (d) EL 200.

by the system, which is equal to the sum of the static head and friction loss of the system. Therefore, an increase in static head results in an increase in required power input or network hydraulic capacity in order to achieve certain hydraulic reliability levels.

[48] The solution space and resulting Pareto-optimal fronts are shown in Figure 6 for four different static heads (i.e., EL 1, 20, 95, and 200 m) and the critical solutions, including the minimum cost solution, the minimum GHG solution, the maximum *s* factor solution, and the zero *s* factor solution for the four systems are summarized in Table 6. The visualization technique used in Figure 6 is similar to the many-objective visual analytics applied by *Fu et al* [2012] in that a color scheme is used. However, instead of representing different values of different objectives for the solutions of a many-objective optimization problem, as has been done by *Fu et al*. [2012], the color scheme is used in this study to better illustrate the shift of the location of the Pareto-optimal front in the solution space and the change in two-objective Pareto-optimality along the three-objective Pareto-optimal front. Therefore, a single solution may be presented by more than one color in Figure 6 if the solution fits into more than one category.

[49] As can be seen in Figure 6, as the static head increases from 1 to 200 m, the Pareto-optimal front gradually shifts from the upper "arm" to the lower "arm" of the U-shaped solution space. Only the "elbow" section of the solution space is always Pareto-optimal due to the tradeoffs between economic cost and GHG emissions, which are independent of the change in static head. This change in the location of the Pareto-optimal front with static head is mainly due to the fact that a single value of the *s* factor can be obtained by either increasing the pumping power input or the pipe capacity, as discussed previously. When there is almost no static head in the system, the total pumping power required is generally low. Under this condition, it is more economic to increase the hydraulic reliability of the system represented by the *s* factor by increasing pumping power compared to increasing pipe capacity and therefore, the smaller networks located on the upper "arm" of the solution space are Pareto-optimal (e.g., the EL 1 system shown in Figure 6a). In contrast, when the static head in the system is large, the total pumping power required is also large. Under this condition, it is more economic to increase the *s* factor by increasing the pipe capacity (i.e., pipe diameter) compared to further increasing pumping power input and therefore, the larger networks located on the lower "arm" of the solution space are Pareto-optimal (e.g., the EL 95 and EL 200 systems shown in Figures 6c and 6d). For systems with medium static heads, such as the EL 20 system shown in Figure 6b, parts of the two "arms" of the solution space can be Pareto-optimal depending on the

**Table 6.** Critical Solutions for Case Study 1 With Different Static Heads

| EL (m) | Solution | PPO[a] | Total Cost ($M) | Total GHG (kt) | $s$ | Pipe Cost ($M) | Station Cost ($M) | Pump Cost ($M) | Operating Cost ($M) | Pipe GHG (kt) | Operating GHG (kt) | $h_f$ (m) | $Q_{in} > Q_{max}$ |
|---|---|---|---|---|---|---|---|---|---|---|---|---|---|
| 1 | Minimum cost | [2,3] | 1.56 | 5 | 0.82 | 1.13 | 0.29 | 0.04 | 0.10 | 1.3 | 4 | 13.2 | Yes |
| | Minimum GHG | [2,2] | 1.82 | 3 | 0.33 | 1.57 | 0.20 | 0.02 | 0.04 | 2.1 | 1 | 2.21 | Yes |
| | Maximum $s$ | [2,2] | 3.15 | 38 | 0.98 | 0.71 | 1.27 | 0.24 | 0.92 | 0.7 | 38 | 170 | Yes |
| | *Zero s*[b] | *NA*[c] | *2.30* | *4* | *0.00* | *2.07* | *0.18* | *0.02* | *0.03* | *3.1* | *1* | *0.50* | *NA* |
| 20 | Minimum cost | [2,2] | 2.19 | 19 | 0.02 | 1.12 | 0.45 | 0.07 | 0.56 | 1.3 | 17 | 13.6 | Yes |
| | Minimum GHG | [2,2] | 2.46 | 17 | 0.26 | 1.57 | 0.36 | 0.05 | 0.49 | 2.1 | 15 | 2.21 | No |
| | Maximum $s$ | [2,2] | 4.23 | 20 | 0.89 | 3.37 | 0.34 | 0.05 | 0.47 | 5.8 | 14 | 0.04 | No |
| | Zero s | [2,1] | 2.20 | 18 | 0.00 | 1.18 | 0.42 | 0.06 | 0.53 | 1.4 | 17 | 10.1 | NA |
| 95 | Minimum cost | [2,2] | 4.56 | 72 | 0.16 | 1.09 | 0.97 | 0.17 | 2.34 | 1.3 | 71 | 15.8 | No |
| | Minimum GHG | [2,3] | 4.86 | 70 | 0.62 | 1.57 | 0.89 | 0.15 | 2.26 | 2.1 | 68 | 2.21 | No |
| | Maximum $s$ | [2,2] | 6.63 | 73 | 0.95 | 3.37 | 0.87 | 0.15 | 2.24 | 5.8 | 67 | 0.04 | No |
| | *Zero s* | *NA* | *4.75* | *79* | *0.00* | *0.89* | *1.14* | *0.21* | *2.51* | *1.0* | *78* | *47.2* | *NA* |
| 200 | Minimum cost | [2,2] | 7.65 | 147 | 0.31 | 1.06 | 1.47 | 0.29 | 4.83 | 1.2 | 146 | 18.4 | No |
| | Minimum GHG | [2,3] | 7.98 | 144 | 0.73 | 1.57 | 1.41 | 0.27 | 4.73 | 2.1 | 142 | 2.21 | No |
| | Maximum $s$ | [2,2] | 9.76 | 147 | 0.96 | 3.37 | 1.40 | 0.27 | 4.72 | 5.8 | 142 | 0.04 | No |
| | *Zero s* | *NA* | *8.16* | *164* | *0.00* | *0.78* | *1.75* | *0.37* | *5.26* | *0.8* | *164* | *101* | *NA* |

[a]PPO, Pareto preference ordering.
[b]Solutions given in italics are not Pareto-optimal solutions.
[c]NA, not applicable.

relative efficiency in increasing the hydraulic reliability via either increasing pumping power or pipe capacity.

[50] The two-objective optimality of the Pareto-optimal solutions also changes with static head. As shown in Tables 3 and 6, the minimum cost solution is the only [2,3]-Pareto-optimal solution for the EL 1 system and all the other Pareto-optimal solutions, including the minimum GHG solution and the maximum $s$ factor solutions, are [2,2]-Pareto-optimal. For the EL 1 system, all of the Pareto-optimal solutions are cost-$s$ optimal, with the solutions located on the upper "arm" also being GHG-$s$ optimal, and the solutions located on the "elbow" also being cost-GHG optimal, as shown in Figure 6a. The maximum $s$ factor solution is the network with the smallest diameter pipe located at the upper end of the upper "arm" of the solution space due to its high pumping power input. The zero $s$ factor solution is located on the lower "arm" of the solution space and is not a Pareto-optimal solution. This indicates that all of the Pareto-optimal solutions of the EL 1 system have higher $Q_{in}$ compared to $Q_{max}$, and therefore, increasing pumping power input is a more efficient way of increasing hydraulic reliability for these networks compared to increasing pipe capacity.

[51] As the static head is increased to 20 m, the solutions located on the lower "arm" become GHG-$s$ optimal. The networks with the smallest diameters (i.e., solutions on the higher end of the upper "arm") are no longer Pareto-optimal; while part of the larger diameter networks on the lower "arm" of the solution space become cost-$s$ optimal. For this EL 20 system, there are no [2,3]-Pareto-optimal solutions, and nearly half of the Pareto-optimal solutions are only [2,1]-Pareto-optimal, as shown in Figure 6b. However, it should be noted that the zero $s$ factor solution is on the Pareto-optimal front and is [2,1]-Pareto-optimal in terms of the economic and environmental objectives.

[52] When a system has high static head, such as the EL 95 and EL 200 systems shown in Figures 6c and 6d, the minimum GHG solution becomes the [2,3]-Pareto-optimal solution. In this case, all Pareto-optimal solutions are cost-$s$ optimal with the solutions located on the lower "arm" also being GHG-$s$ optimal and the solutions located on the "elbow" also being cost-GHG optimal. In addition, the network with the largest diameter is the maximum $s$ factor solution due to its large pipe capacity. Similarly to the EL 1 system, the zero $s$ factor solution is not on the Pareto-optimal front, as it is located on the upper "arm" of the solution space. This indicates that the Pareto-optimal solutions of systems with high static head have lower $Q_{in}$ compared to $Q_{max}$, and therefore, increasing pipe capacity is a more efficient way of increasing hydraulic reliability for these networks compared to increasing pumping power input.

[53] In order to compare the results of the second and third case studies with those of the four case study 1 systems with different static heads, the two-objective Pareto-optimality of the [2,2]-Pareto-optimal solutions of case studies 2 and 3 are plotted in Figure 7. The critical solutions of case studies 2 and 3 are summarized in Table 7. It can be seen from Figures 6 and 7 that case study 2 generally falls into the category of having medium static head (e.g., the EL 20 system of case study 1). First of all, there are no [2,3]-Pareto-optimal solutions for case study 2 and the zero $s$ factor solution is a [2,1]-Pareto-optimal solution

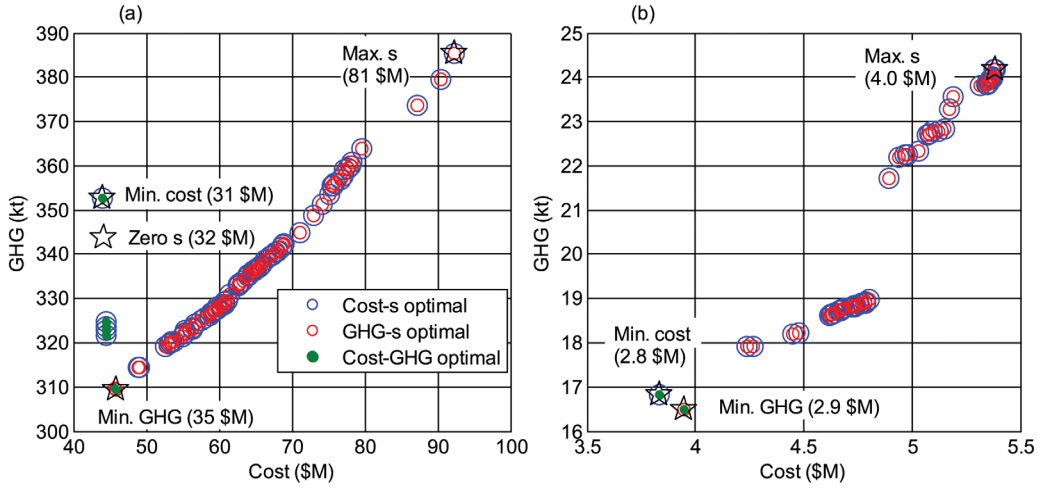


**Figure 7.** Two-objective optimality of [2,2]-Pareto-optimal solutions for (a) case studies 2 and (b) 3 (Note: the number in the parentheses indicates the cost of the pipes).

(see Table 5), which is consistent with the results of the EL 20 system. In addition, the minimum cost solution of case study 2 satisfies the condition of $Q_{in}$ being greater than $Q_{max}$ while all other solutions that are more expensive than the zero *s* factor solution in Figure 7a satisfy the condition of $Q_{in}$ being less than $Q_{max}$. This finding is consistent with the elevations of the demand nodes in the system, which are between 15 and 25 m [*Duan et al*., 1990]. The major difference between the results from case study 2 and those from the EL 20 system shown in Figure 6b is that the Pareto-optimal front of case study 2 does not extend deeply into the upper "arm" of the solution space. This is mainly because case study 2 is a looped network and therefore, it is less likely to have network configurations with very small pipe capacity (i.e., the solutions on the upper "arm" of the solution space in Figure 6). In addition, the fact that the case study 2 solutions on the "elbow" section are mostly [2,2]-Pareto-optimal rather than [2,1]-Pareto-optimal, as is the case for the EL 20 system, indicates that case study 2 has a relatively higher static-head-to-friction-loss ratio compared to the EL 20 system, which makes the Pareto-optimal front of case study 2 closer to that of the EL 95 system.

[54] The case study 3 network, which has a static head of about 70 m, falls into the category of having high static head (e.g., similar to the EL 95 and EL 200 systems of case study 1). This is indicated, apart from the two-objective optimality shown in Figure 7b, by the fact that the zero *s* factor solution is not located on the Pareto-optimal front. In addition, all of the Pareto-optimal solutions, including the minimum cost solution, satisfy the condition of $Q_{in}$ being less than $Q_{max}$, as shown in Table 7. The only difference between the results obtained from case study 3 and those from the high static head systems of case study 1 is that the minimum GHG solution of case study 3 is only [2,2]-Pareto-optimal, rather than [2,3]-Pareto-optimal (see Tables 5 and 7). However, for real-world systems with many decision variables, the solution space is likely to be more rugged and there is therefore no guarantee that the globally Pareto-optimal solutions can be found. Therefore, it is highly likely that a [2,3]-Pareto-optimal solution that is optimal in terms of all three pairs of the three objectives does not exist for case study 3 or was not found in the optimization process.

### 4.3. Practical Implications

[55] Based on the results obtained from the three case studies, a number of general conclusions can be drawn to guide the practical design of WDSs involving pumping or WTSs when considering the economic objective of minimizing the total cost, the environmental objective of minimizing GHG emissions and the hydraulic reliability objective of maximizing the *s* factor. First of all, it can be concluded that the solution space of WDS design optimization considering the three objectives manifests itself as a U-shaped curve in the 3-D space. The "elbow" section (viewed form the cost-GHG orientation) of the curve is controlled by the tradeoffs between the economic and environmental objectives; while the upper and lower "arms" of the curve (viewed form the cost-GHG orientation) are determined by the tradeoffs between the hydraulic reliability objective and the other two objectives.

[56] The location of the Pareto-optimal front on the solution space is often case study dependent. For real-world systems, the Pareto-optimal front is often located on the "elbow" section and the lower "arm" of the solution space. For real-world WDSs, this is because they are often looped, and therefore generally have a higher pipe capacity compared with networks with a treed structure. For real-world WTSs, this is because they often need to pump against a significant amount of static head, which makes it more economic to increase the hydraulic reliability of the system by increasing pipe capacity. Therefore, the Pareto-optimal fronts of real-world systems considering the three objectives often have an unbalanced V shape, as shown in Figure 7. The solution at the top of the left-hand side of the V shape is often the minimum cost solution, the solution at the bottom of the V shape is the minimum GHG solution, and the solution at the end of the right-hand side of the V shape is the maximum *s* factor solution. The solutions on the left-hand side of the V shape (i.e., solutions that are cheaper than the minimum GHG solutions) are cost-GHG

**Table 7.** Critical Solutions for Case Studies 2 and 3

| Case Study | Solution | PPO[a] | Total Cost ($M) | Total GHG (kt) | *s* | Pipe Cost ($M) | Station Cost ($M) | Pump Cost ($M) | Operating Cost ($M) | Pipe GHG (kt) | Operating GHG (kt) | $Q_{in} > Q_{max}$ |
|---|---|---|---|---|---|---|---|---|---|---|---|---|
| 2 | Minimum cost | [2,2] | 43.98 | 353 | 0.01 | 31.02 | 2.36 | 0.53 | 10.08 | 37.9 | 315 | Yes |
| | Minimum GHG | [2,2] | 45.91 | 309 | 0.05 | 34.88 | 1.90 | 0.41 | 8.71 | 47.0 | 262 | No |
| | Maximum *s* | [2,2] | 92.27 | 385 | 0.83 | 81.42 | 1.86 | 0.40 | 8.59 | 127.6 | 258 | No |
| | Zero *s* | [2,1] | 44.14 | 344 | 0.00 | 31.54 | 2.26 | 0.51 | 9.84 | 38.5 | 305 | NA[b] |
| 3 | Minimum cost | [2,2] | 3.83 | 17 | 0.10 | 2.75 | 0.52 | 0.08 | 0.48 | 3.8 | 13 | No |
| | Minimum GHG | [2,2] | 3.95 | 16 | 0.06 | 2.90 | 0.51 | 0.08 | 0.46 | 3.9 | 13 | No |
| | Maximum *s* | [2,2] | 5.38 | 24 | 0.63 | 3.99 | 0.68 | 0.11 | 0.60 | 6.6 | 18 | No |

[a]PPO, Pareto preference ordering
[b]NA, not applicable.

optimal and have relatively lower pipe capacities compared with the solutions on the right-hand side of the V shape (i.e., solutions that are more expensive than the minimum GHG solution), which are often GHG-*s* optimal. Most solutions on the Pareto-optimal front are optimal in terms of the economic and reliability objectives.

[57] In addition, Pareto preference ordering has been found to be useful in assisting decision making by prioritizing "superior" solutions. Based on Pareto preference ordering, the Pareto-optimal solutions with the best objective function values (i.e., the minimum cost and GHG solutions and the maximum *s* factor solution) are generally [2,2]-Pareto-optimal and therefore more desirable. Due to the rugged nature of the solution space of real-world systems, the [2,3]-Pareto-optimal solution cannot always be found. However, if a [2,3]-Pareto-optimal solution does exist, it should be the minimum GHG solution. Furthermore, due to the shape of the Pareto-optimal front of real-world systems, two solutions having the same GHG emissions but different cost-*s* tradeoffs exist. The solution on the left-hand side of the minimum GHG solution has a lower cost but is less hydraulically reliable; while the solution on the right-hand side of the minimum GHG solution is more expensive but more hydraulically reliable. These solutions are both [2,2]-Pareto-optimal based on Pareto preference ordering. The final decision regarding the preference of these solutions needs to be made using expert knowledge and considering the requirements of the specific design, such as budget and reliability requirements.

## 5. Summary and Conclusions

[58] The study presented in this paper investigates the tradeoffs among the economic objective of minimizing total cost, the environmental objective of minimizing total GHG emissions, and the reliability objective of maximizing surplus power factor (or the *s* factor) for water distribution systems (WDSs) involving pumping or water transmission systems (WTSs). The tradeoffs among these three objectives have not been examined together previously. One reason for this is that traditionally used measures of hydraulic reliability cannot be used as an objective for the optimization of WDSs where water is pumped into storages. However, these systems are major contributors of GHG emissions in the water industry. In order to overcome this dilemma, the hydraulic reliability/resilience measure introduced by *Wu et al*. [2011] is used as the hydraulic reliability measure in this study, as it makes use of the concept of the surplus power factor (or *s* factor) of *Vaabel et al*. [2006], the calculation of which does not require the value of the pressure head at the outlet of the system and can therefore be used as an objective for systems that pump into storages. This enables hydraulic reliability to be included as an objective together with cost and GHG minimization objectives for the optimization of WDSs.

[59] The main aim of this paper is to gain a good understanding of the generic nature of tradeoffs among the three objectives for systems that involve pumping into storage facilities, which are of primary interest from a GHG emission minimization perspective. This aim is achieved via three case studies, including two hypothetical case studies form the literature and one real-world case study. Based on the results from the case studies, it is found that the shape of the solution space formed by the three objectives for WDSs involving pumping or WTSs is always a U-shaped curve (with an upper "arm," an "elbow" section and a lower "arm"), rather than a surface in the three-dimensional objective space. This is due to the fact that the same hydraulic reliability level represented by the *s* factor can be achieved by either increasing pumping power or pipe capacity.

[60] The location of the Pareto-optimal front in this solution space depends on the pipe capacity or static head of the system. For real-world WDSs, which are often looped, and WTSs, which often pump against relatively high static head compared to friction loss, it is more economic to increase the hydraulic reliability of the system by increasing pipe capacity (i.e., pipe diameters) rather than by increasing pumping power. Therefore, the Pareto-optimal fronts of real-world systems considering the three objectives are often located on the "elbow" section and the lower "arm" of the solution space. The two-objective optimality of these Pareto-optimal solutions is often case study dependent. However, based on Pareto preference ordering, the solutions with the best objective function values (i.e., the minimum cost solution, the minimum GHG solution, and the maximum *s* factor solution), especially the minimum GHG solution, often have more "balanced" objective function values and therefore, are more desirable. In addition, for real-world systems, solutions with similar GHG emissions but different cost-reliability tradeoffs often exist, which requires engineering judgment in order to select the most preferred solution.

[61] In conclusion, the findings of this study provide useful insights into the tradeoffs among the economic, environmental, and hydraulic reliability of WDSs involving pumping or WTSs, which can be used to guide the design

of WDSs considering these three objectives in practice. Based on the findings of this study, it is clear that the trade-offs that need to be considered in practice are restricted to a relatively small region of the total solution space. Pareto preference ordering has been found to be able to effectively reduce the number of candidate solutions obtained from multiobjective optimization and assist the final decision making by prioritizing more desirable solutions. However, the final decision still needs to be made in conjunction with expert knowledge and the specific design requirements of the system.

[62] **Acknowledgments.** This research was supported by resources supplied by eResearch SA, South Australia. The authors would like to thank Xiaojian Wang from SA Water for providing information on the third case study. The authors also acknowledge the three anonymous reviewers, whose input has helped to improve the quality of this paper significantly.

## References

Ambrose, M. D., G. D. Salomonsson, and S. Burn (2002), Piping systems embodied energy analysis, CMIT Doc. 02/302, CSIRO Manufact. and Infrastruct. *Technol., Highett, Australia*.

Atiquzzaman, M., S.-Y. Liong, and X. Yu (2006), Alternative decision making in water distribution network with NSGA-II, *J. Water Resour. Plann. Manage.*, *132*(2), 122–126, doi:org/10.1061/(ASCE)0733–9496(2006)132:2(122).

Dandy, G. C., A. Roberts, C. Hewitson, and P. Chrystie (2006), Sustainability objectives for the optimization of water distribution networks, paper presented at Proceedings of 8th Annual Water Distribution Systems Analysis Symposium, ASCE, Cincinnati, Ohio, Aug.

Dandy, G. C., A. Bogdanowicz, J. Craven, A. Maywald, and P. Liu (2008), Optimizing the sustainability of water distribution systems, paper presented at 10th Annual Symposium on Water Distribution Systems Analysis, ASCE, Kruger Natl. Park, South Africa, 17–20 Aug.

Das, I. (1999), A preference ordering among various Pareto optimal alternatives, *Struct. Optim*, *18*(1), 30–35, doi:10.1007/bf01210689.

Deb, K., S. Agrawal, A. Pratap, and T. Meyarivan (2000), A fast elitist non-dominated sorting genetic algorithm for multi-objective optimization: NSGA-II, in *Parallel Problem Solving from Nature–PPSN VI*, edited by M. Schoenauer et al., pp. 849–858, Springer, Berlin.

Duan, N., L. W. Mays, and K. E. Lansey (1990), Optimal reliability-based design of pumping and distribution systems, *J. Hydraul. Eng.*, *116*(2), 249–268, doi:org/10.1061/(ASCE)0733–9429(1990)116:2(249).

Farmani, R., G. Walters, and D. Savic (2006), Evolutionary multi-objective optimization of the design and operation of water distribution network: Total cost vs. reliability vs. water quality, *J. Hydroinformatics*, *8*(3), 165–179.

Fearnside, P. M. (2002), Time preference in global warming calculations: A proposal for a unified index, *Ecol. Econ.*, *41*(1), 21–31.

Filion, Y. R., H. L. MacLean, and B. W. Karney (2004), Life-cycle energy analysis of a water distribution system, *J. Infrastruct. Syst.*, *10*(3), 120–130.

Fu, G., and Z. Kapelan (2011), Fuzzy probabilistic design of water distribution networks, *Water Resour. Res.*, *47*(5), W05538, doi:10.1029/2010WR009739.

Fu, G., Z. Kapelan, J. Kasprzyk, and P. Reed (2012), Optimal design of water distribution systems using many-objective visual analytics, *J. Water Resour. Plann. Manage.*, doi:10.1061/(asce)wr.1943–5452.0000311.

Gessler, J., and T. M. Walski (1985), Water distribution system optimization, *Tech. Rep. EL-85-11*, Dep. of the Army, U.S. Army Corps of Eng., Washington, D. C.

Ghimire, S. R., and B. D. Barkdoll (2007), Incorporating environmental impact in decision making for municipal drinking water distribution systems through eco-efficiency analysis, paper presented at Proceedings of the World Environmental and Water Resources Congress 2007: Restoring Our Natural Habitat, Tampa, Fla, 15–19 May.

Giustolisi, O., D. Laucelli, and D. A. Savic (2006), Development of rehabilitation plans for water mains replacement considering risk and cost-benefit assessment, *Civil Eng. Environ. Syst.*, *23*(3), 175–190, doi:10.1080/10286600600789375.

Halhal, D., G. A. Walters, D. Ouazar, and D. A. Savic (1997), Water network rehabilitation with structured messy genetic algorithm, *J. Water Resour. Plann. Manage.*, *123*(3), 137–146.

Herstein, L. M., Y. R. Filion, and K. R. Hall (2009), EIO-LCA based multi-objective design of water distribution systems with NSGA-II, paper presented at Computing and Control in the Water Industry 2009 "Integrating Water Systems," London, U. K., 1–3 Sept.

Ilich, N., and S. P. Simonovic (1998), Evolutionary algorithm for minimization of pumping cost, *J. Comput. Civil Eng.*, *12*(4), 232–240.

Jayaram, N., and K. Srinivasan (2008), Performance-based optimal design and rehabilitation of water distribution networks using life cycle costing, *Water Resour. Res.*, *44*(1), W01417, doi:10.1029/2006WR005316.

Jourdan, L., D. W. Corne, D. Savic, and G. Walters (2005), LEMMO: Hybridising rule induction and NSGA II for multi-objective water systems design, paper presented at CCWI. The Eight International Conference on Computing and Control for the Water Industry (CCWI), University of Exeter, Exeter, UK, 5–7 Sept. 2005.

Kapelan, Z. S., D. A. Savic, and G. A. Walters (2005), Multiobjective design of water distribution systems under uncertainty, *Water Resour. Res.*, *41*(11), W11407, doi:10.1029/2004WR003787.

Keedwell, E., and S.-T. Khu (2004), Hybrid Genetic algorithms for multi-objective optimisation of water distribution networks, in *Genetic and Evolutionary Computation–GECCO 2004*, edited by K. Deb, pp. 1042–1053, Springer, Berlin, doi:10.1007/978-3-540–24855-2_115.

Khu, S. T., and H. Madsen (2005), Multiobjective calibration with Pareto preference ordering: An application to rainfall-runoff model calibration, *Water Resour. Res.*, *41*(3), W03004, doi:10.1029/2004WR003041.

Li, D., T. Dolezal, and Y. Y. Haimes (1993), Capacity reliability of water distribution networks, *Reliab. Eng. Syst. Safety*, *42*, 29–38.

Nitivattananon, V., E. C. Sadowski, and R. G. Quimpo (1996), Optimization of water supply system operation, *J. Water Resour. Plann. Manage.*, *122*(5), 374–384.

Ormsbee, L. E., and K. E. Lansey (1994), Optimal control of water supply pumping systems, *J. Water Resour. Plann. Manage.*, *120*(2), 237–252, doi:10.1061/(ASCE)0733–9496(1994)120:2(237).

Pezeshk, S., and O. J. Helweg (1996), Adaptive search optimisation in reducing pump operating costs, *J. Water Resour. Plann. Manage.*, *122*(1), 57–63.

Prasad, T. D., and N.-S. Park (2004), Multiobjective genetic algorithms for design of water distribution networks, *J. Water Resour. Plann. Manage.*, *130*(1), 73–82.

Rossman, L. A. (2000), EPANET2, EPA/600/R-00/057, Water Supply and Water Resources Division, Natl. Risk Management Res. Lab., Off. of Res. Dev., USEPA, Cincinnati, Ohio.

Savic, D. (2002), Single-objective vs. multiobjective optimisation for integrated decision support, in *Integrated Assessment and Decision Support: Proceedings of the First Biennial Meeting of the International Environmental Modelling and Software Society*, edited by A. E. Rizzoli and A. J. Jakeman, pp. 7–12, Lugano, Switzerland.

Schneiter, C. R., Y. Y. Haimes, D. Li, and J. H. Lambert (1996), Capacity reliability of water distribution networks and optimum rehabilitation decision making, *Water Resour. Res.*, *32*(7), 2271–2278.

Simpson, A. R., G. C. Dandy, and L. J. Murphy (1994), Genetic algorithms compared to other techniques for pipe optimization, *J. Water Resour. Plann. Manage.*, *120*(4), 423–443.

The Department of Climate Change (2008), National greenhouse accounts (NGA) factors, The Dep. of Clim. Change, Commonwealth of Australia, Canberra, Australia.

Todini, E. (2000), Looped water distribution networks design using a resilience index based heuristic approach, *Urban Water*, *2*, 115–122.

Tolson, B. A., H. R. Maier, A. R. Simpson, and B. J. Lence (2004), Genetic algorithms for reliability-based optimization of water distribution systems, *J. Water Resour. Plann. Manage.*, *130*(1), 63–72.

Ulanicki, B., J. Kahler, and H. See (2007), Dynamic optimization approach for solving an optimal scheduling problem in water distribution systems, *J. Water Resour. Plann. Manage.*, *133*(1), 23–32.

Vaabel, J., L. Ainola, and T. Koppel (2006), Hydraulic power analysis for determination of characteristics of a water distribution system, paper presented at 8th Annual Water Distribution Systems Analysis Symposium, Cincinnati, Ohio, 27–30 Aug.

van Zyl, J. E., D. A. Savic, and G. A. Walters (2004), Operational optimization of water distribution systems using a hybrid genetic algorithm, *J. Water Resour. Plann. Manage.*, *130*(2), 160–170.

Walski, T. M., J. Gessler, and J. W. Sjostrom (1988), Selecting optimal pipe sizes for water distribution systems, *J. Am. Water Works Assoc.*, *80*(2), 35–39.

Water Services Association of Australia (2002), *Water Supply Code of Australia: WSA 03–2002*, Water Serv. Assoc. of Australia, Melbourne, Australia.

Wu, W., A. R. Simpson, and H. R. Maier (2008), Multi-objective genetic algorithm optimisation of water distribution systems accounting for sustainability, paper presented at Water Down Under 2008: Incorporating 31st Hydrology and Water Resources Symposium and the 4th International Conference on Water Resources and Environment Research (ICWRER), Adelaide, Australia.

Wu, W., A. R. Simpson, and H. R. Maier (2010a), Accounting for greenhouse gas emissions in multiobjective genetic algorithm optimization of water distribution systems, *J. Water Resour. Plann. Manage.*, *136*(2), 146–155, doi:10.1061/(ASCE)WR.1943–5452.0000020.

Wu, W., H. R. Maier, and A. R. Simpson (2010b), Single-objective versus multiobjective optimization of water distribution systems accounting for greenhouse gas emissions by carbon pricing, *J. Water Resour. Plann. Manage.*, *136*(5), 555–565, doi:org/10.1061/(ASCE)WR.1943–5452.0000072.

Wu, W., H. R. Maier, and A. R. Simpson (2011), Surplus power factor as a resilience measure for assessing hydraulic reliability in water transmission system optimization, *J. Water Resour. Plann. Manage.*, *137*(6), 542–546, doi:10.1061/(ASCE)WR.1943–5452.0000138.

Wu, W., H. R. Maier, and A. R. Simpson (2012a), Sensitivity of optimal tradeoffs between cost and greenhouse gas emissions for water distribution systems to electricity tariff and generation, *J. Water Resour. Plann. Manage.*, *138*(2), 182–186, doi:10.1061/(ASCE)WR.1943–5452.0000169.

Wu, W., A. R. Simpson, H. R. Maier, and A. Marchi (2012b), Incorporation of variable-speed pumping in multiobjective genetic algorithm optimization of the design of water transmission systems, *J. Water Resour. Plann. Manage.*, *138*(5), 543–552, doi:10.1061/(ASCE)WR.1943–5452.000019.